Reagents and apparatus

Iron chloride hexahydrate ($FeCl_3 \cdot 6H_2O$, 99%), pyrrole, titanium butoxide (TBOT, 99%), terephthalic acid (H_2BDC, 99%), methyl orange (MO), Sodium dihydrogen phosphate ($NaH_2PO_4 \cdot 2H_2O$, AR) and disodium phosphate dodecahydrate ($Na_2HPO_4 \cdot 12H_2O$, 99%) were purchased from Aladdin Chemical Reagent Co., Ltd. Manganese acetate tetrahydrate ($Mn(COO)_2 \cdot 4H_2O$, 99%) was purchased from Jinshan Xingtar Chemical Factory. (Shanghai, China).

SEM images were obtained on JEOL JSM-7610F Plus (Japan); the powder XRD spectra and XPS spectra were recorded by D8 advances X-ray diffractometer (Bruker, Germany); the FTIR spectra of the powder were tested by VERTEX 70 spectrum FTIR instrument (Bruker, Germany). Electrochemical tests were performed on CHI 660E electrochemical workstation (CHI Instruments, Shanghai, China). The electrochemical system consists of a working electrode (glass carbon electrode, GCE), a reference electrode (saturated calomel electrode) and a counter electrode (platinum electrode).

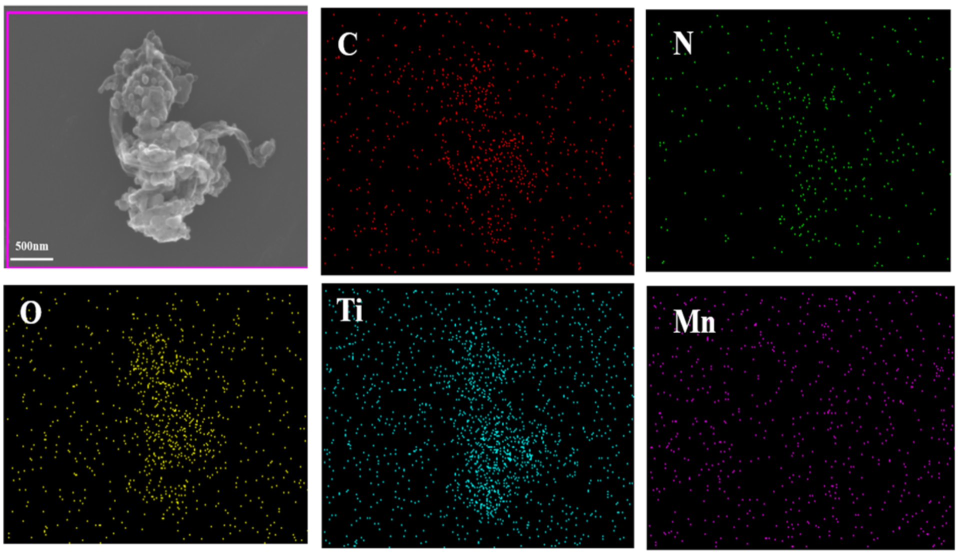

Fig. S1 Elemental mapping image of $MnO/TiO_2/C/N$-CNTs.

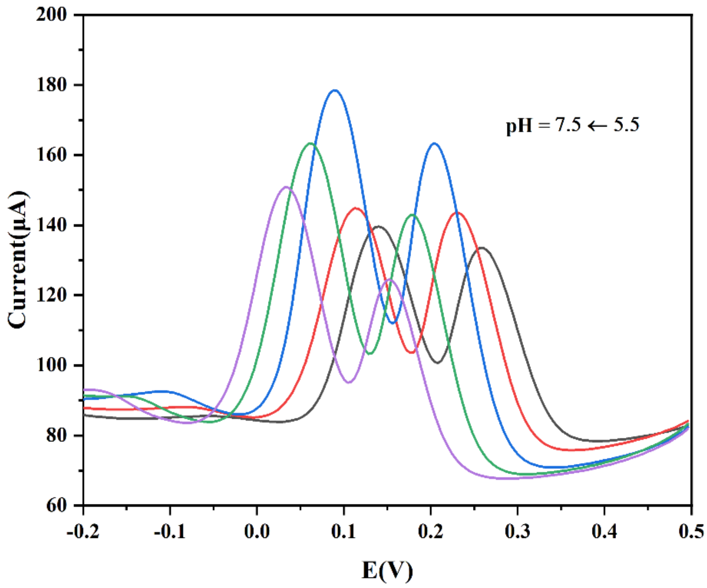

Fig. S2 The changes of oxidation peak current and potential of CC and HQ at different pH values

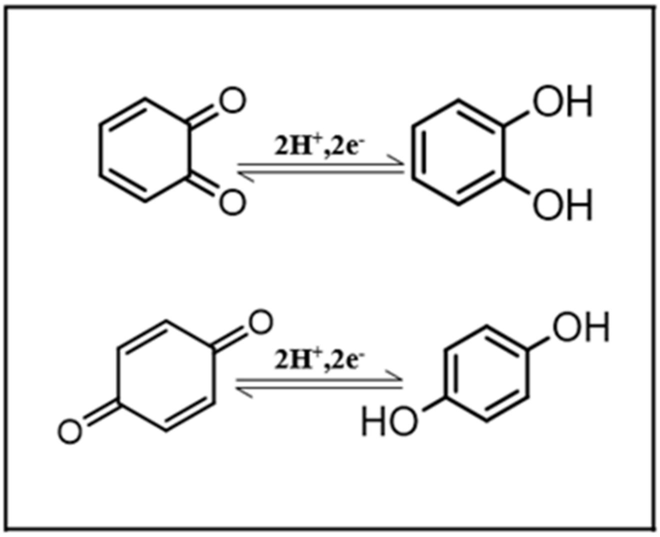

Fig. S3 Principles of CC and HQ reactions at $MnO/TiO_2/C/N$-CNTs/GCE surface.

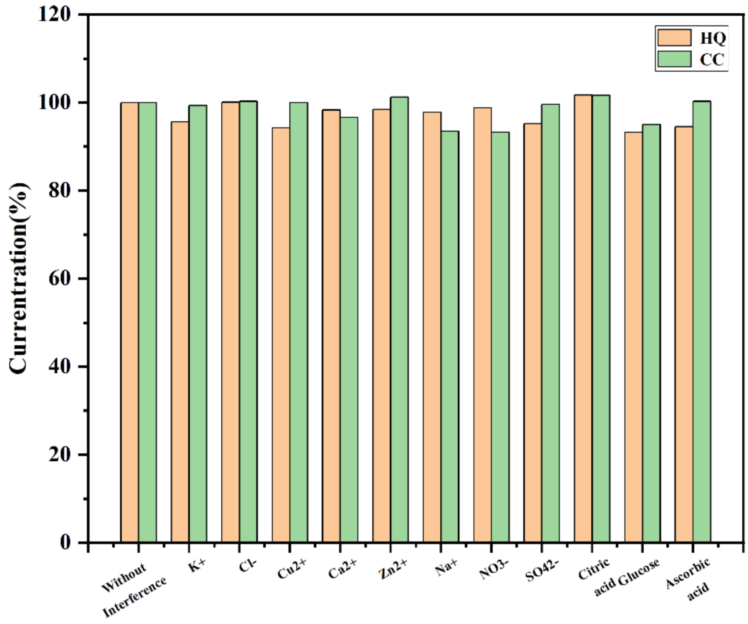

Fig. S4 Effects of different interfering substances on the detection of CC and HQ at $MnO/TiO_2/C$/N-CNTs/GCE.

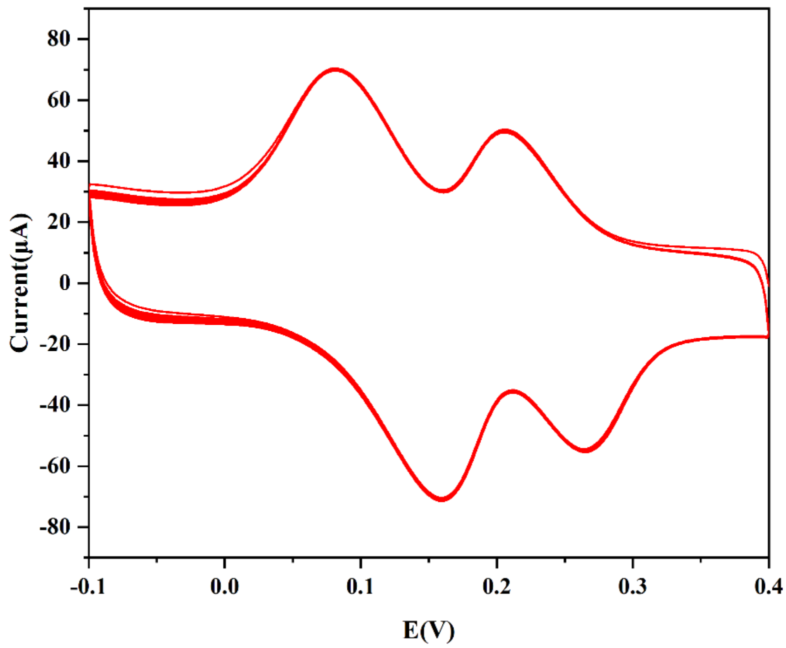

Fig. S5 CV curves of $MnO/TiO_2/C$/N-CNTs/GCE were scanned in 0.1 M PBS containing 50 μM CC and 50 μM HQ for 50 consecutive cycles.

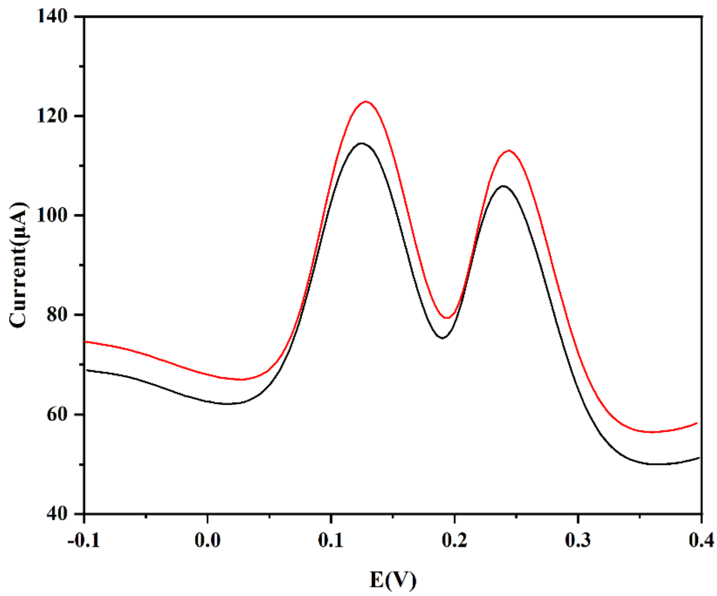

Fig. S6 DPV curves of CC and HQ at the MnO/TiO2/C/N-CNTs/GCE before and after 7 days of storage at 4 °C in a refrigerator.

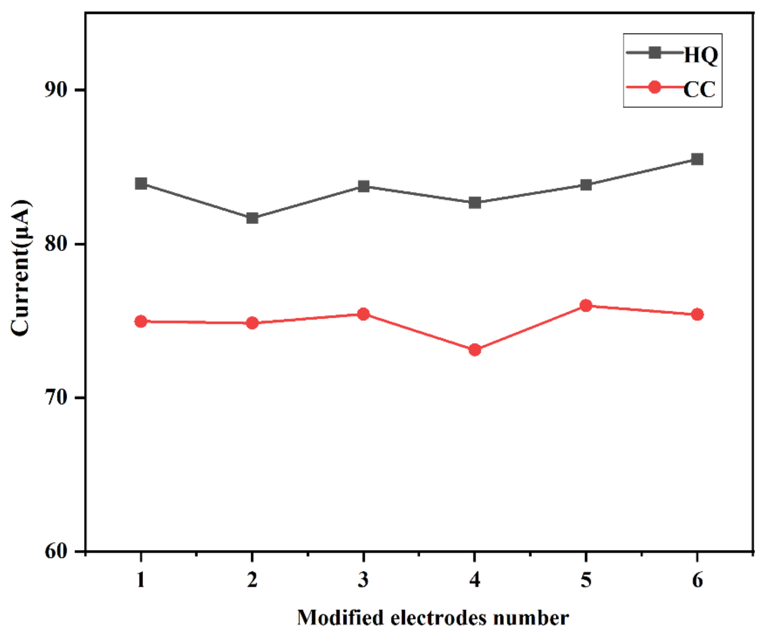

Fig. S7 DPV response currents of the six modified electrodes to CC and HQ.